

Equation (16) is now considered for the heat conduction through a thin fin under the assumption that the conductivity-thickness product varies according to

$$k_f t = (k_f t)_b (x/x_b)^s \quad (26)$$

where  $s$  is the prescribed fin shape exponent. The substitution of Eqs. (26), (23), and (19) into Eq. (16) yields

$$n(s-n-1)(k_f t/x^2) + \frac{1}{2}[(3+4m)n-1]^{1/2}(k Rax^{1/2}/x) = 0 \quad (27)$$

The foregoing equation suggests the existence of similarity solutions, namely

$$\begin{aligned} \left(\frac{kx}{k_f t}\right) Rax^{1/2} &= \frac{kx_b}{(k_f t)_b} Rax_b^{1/2} \\ &= \frac{2(4-3s)(3-2s)}{[(3+4m)(3-2s)-1]^{1/2}} = Ncc \end{aligned} \quad (28a)$$

where

$$n = 3 - 2s \quad (28b)$$

Therefore, the constraint described by Eq. (24a) is equivalent to

$$s < 4/3 \quad (29)$$

Once the thermal stratification parameter  $m$  and the fin shape exponent  $s$  for the conductivity-thickness product are given, the so-called "conduction/convection parameter"  $Ncc$  may readily be calculated from the last expression on the right-hand side of Eq. (28a). Thus, the unknown value  $x_b$  can be determined from Eq. (16a) as

$$x_b = \left[ \left( \frac{\alpha \nu}{Kg\beta \Delta T_{wb}} \right)^{1/2} \frac{(k_f t)_b Ncc}{k} \right]^{2/3} \quad (30)$$

The substitution of Eqs. (22), (23), and (28) into Eq. (19) leads to the following closed-form expression for the isotherms:

$$\begin{aligned} y/x_b &= - \frac{kx_b/(k_f t)_b}{(4-3s)(3-2s)} \\ &\left( \frac{x}{x_b} \right)^{2-s} \ln \left[ \left( \frac{T - T_c}{\Delta T_{wb}} \right) \left( \frac{x}{x_b} \right)^{3-2s} - m \right] \end{aligned} \quad (31)$$

In order to illustrate the temperature fields within the porous medium, the isotherms were obtained for the case of an infinitely long copper fin with constant thermal conductivity and thickness. The case was previously treated by Pop et al.<sup>6</sup> for the constant ambient temperature. Computations were carried out assuming  $k_f = 376.8$  W/m°C,  $t = 0.005$  m,  $T_{wb} = 200^\circ\text{C}$ ,  $K = 10^{-8}$  m<sup>2</sup>,  $k = 2.428$  W/m°C,  $g = 9.8$  m/s<sup>2</sup>,  $\beta = 1.8 \times 10^{-4}/^\circ\text{C}$ ,  $\nu = 0.27 \times 10^{-6}$  m<sup>2</sup>/s,  $\alpha = 0.63 \times 10^{-6}$  m<sup>2</sup>/s, and the constant ambient temperature  $T_c = 15^\circ\text{C}$  ( $m = 0$ ). The resulting isotherms are plotted in Fig. 4a, which indicates a close agreement between the present solution and the exact solution.<sup>6</sup> As pointed out by Pop et al.,<sup>6</sup> the isotherms near the base curve back as a result of a strong flow acceleration there.

When the base is heated up to a high temperature, the effect of the thermal stratification within the porous medium may no longer be negligible. Thus, illustrative calculations were made with the same base temperature but with the thermal stratification parameter  $m = 1$  and the reference temperature  $T_c = T_e|_{x \rightarrow \infty} = 15^\circ\text{C}$ . Even for the same fin temperature distributions, the isotherms, as plotted in Fig. 4b, indicate a

pattern quite different from that in Fig. 4a. These isotherms do not curve back toward the base but extend horizontally away from the fin surface as a result of the thermal stratification. In this sense, the previous solution for the constant temperature should be regarded as somewhat overidealized.

## References

- <sup>1</sup>Wooding, R.A., "Convection in a Saturated Porous Medium at Large Rayleigh Number or Peclet Number," *Journal of Fluid Mechanics*, Vol. 15, 1963, pp. 527-544.
- <sup>2</sup>Cheng, P., "Heat Transfer in Geothermal Systems," *Advances in Heat Transfer*, Vol. 14, 1978, pp. 1-105.
- <sup>3</sup>Cheng, P. and Minkowycz, W.J., "Free Convection about a Vertical Flat Plate Embedded in a Saturated Porous Medium with Application to Heat Transfer from a Dike," *Journal of Geophysics Research*, Vol. 82, 1977, pp. 2040-2044.
- <sup>4</sup>Bejan, A., *Convection Heat Transfer*, Wiley, New York, 1984, pp. 367-371.
- <sup>5</sup>Bejan, A. and Anderson, R., "Heat Transfer Across a Vertical Impermeable Partition Imbedded in a Porous Medium," *International Journal of Heat Mass Transfer*, Vol. 24, 1981, pp. 1237-1245.
- <sup>6</sup>Pop, I., Sunada, J.K., Cheng, P., and Minkowycz, W.J., "Conjugate Free Convection from Long Vertical Plate Fins Embedded in a Porous Medium at High Rayleigh Numbers," *International Journal of Heat Transfer*, Vol. 28-9, 1985, pp. 1629-1636.
- <sup>7</sup>Nakayama, A. and Koyama, H., "An Integral Treatment of Laminar and Turbulent Film Condensation on Bodies of Arbitrary Geometrical Configuration," *Journal of Heat Transfer*, Vol. 107, 1985, pp. 417-423.
- <sup>8</sup>Nakayama, A., Shenoy, A.V., and Koyama, H., "An Analysis for Forced Convection Heat Transfer from External Surfaces to Non-Newtonian Fluids," *Wärme Stoffübertragung*, Vol. 20, 1986, pp. 219-227.

## Gas Particle Radiator

Donald L. Chubb\*

NASA Lewis Research Center, Cleveland, Ohio

## Introduction

HIGH specific power (power radiated/radiator mass), small area, and long lifetime are the desirable characteristics of a space radiator. These characteristics will be attained if a low mass and high emissivity  $\epsilon_T$  that is stable for long periods (7-10 years), can be achieved.

For a tube-type radiator (either a heat pipe or a pumped loop) high emissivity ( $\epsilon > 0.8$ ) is achieved by the use of emissive coatings. Adhesion and emissive stability of these coatings must be obtained for long periods of time if a tube-type radiator is to be a successful space radiator. Generally, the largest mass portion of a tube radiator is the armor that must be used to protect it from meteoroid penetration.

The gas particle radiator (GPR) is a new concept that has the potential for a long lifetime and high emissivity with lower mass than tube radiators. Figure 1 is a conceptual drawing of the GPR. A gas which contains a suspension of fine particles is contained in a sealed volume between the tube radiator and an outer window that are separated by a distance,  $D$ . On start-up of the radiator, a temperature gradient will exist across the gas. This temperature gradient will induce a gas flow that will distribute the particles throughout the gas. However, this will have to be demonstrated for a successful GPR. In the

Received Aug. 12, 1985; revision submitted June 27, 1986. Copyright © 1987 American Institute of Aeronautics and Astronautics, Inc. No copyright is asserted in the United States under Title 17, U.S. Code. The U.S. Government has a royalty-free license to exercise all rights under the copyright claimed herein for Governmental purposes. All other rights are reserved by the copyright owner.

\*Research Engineer. Member AIAA.

microgravity of space the particles should remain in suspension. If the window is transparent to the emitted radiation, the gas particle mixture will yield a high, stable emissivity. Past investigations<sup>1</sup> of a soot-containing flame that is similar to the gas particle mixture of the GPR, have yielded large emissivities. Obtaining high emissivity without the use of emissive coatings is a major advantage of the GPR.

It would appear that the addition of the gas-particle mixture plus a surrounding window will result in a larger mass for the GPR than a tube radiator. However, the addition of the window "bumper" will provide meteoroid protection for the emitting tube. This window bumper means the combined thickness (window + tube) may be significantly less than the tube-only thickness and still provide the same meteoroid protection.<sup>2,3</sup> Therefore, the GPR may have a lower mass than a tube radiator.

The major problem for the GPR is finding a suitable window material. As will be shown, it is the window transmittance that limits the emissivity. There are suitable choices for the gas and particle materials; however, there is a need to experimentally verify the emissivity predicted in this study.

Suitable window materials and a verified emissivity are the critical issues for the GPR. However, even if these issues can be resolved satisfactorily, other design problems will also have to be solved. It will be necessary to provide a seal between the window and the radiating surface. Also, provision will have to be made for the difference in thermal expansion of the window material and the metallic radiating surface material.

### Emissivity of Gas Particle Radiator

A number of studies (summarized in Ref. 1) of the emittance of soot-containing gases have been carried out. These investigations yield large emittances for modest amounts of soot concentration. Seeding with small particles has also been proposed to increase gas absorption of incident radiation<sup>4</sup> or as a means of shielding a surface from incident radiation.<sup>5</sup> The success of the GPR depends on large emittance (or absorption) of the gas-particle mixture. In Ref. 4 large absorption was measured as a function of wavelength,  $\lambda$ , in the range  $0.2 \leq \lambda \leq 1 \mu\text{m}$  for carbon, aluminum oxide, hafnium carbide, and tungsten particles suspended in water. Particle diameters ranged from 0.02 to  $2 \mu\text{m}$ .

The derivation for the total emissivity,  $\epsilon_T$  for the GPR is presented in Ref. 6. The most important approximations used in that derivation are that the gas, particles, and radiator surface are at the same temperature,  $T_p$ , and the absorption coefficient,  $k_\lambda^g$ , of the gas-particle medium is uniform and is determined by the particle optical properties. It is assumed that the gas is transparent to the emitted radiation. Also, the emissivity of the radiator surface,  $\epsilon_p$ , is neglected. To obtain the largest emissivity with the minimum fraction of solid particles it is necessary to use particles of small radius,<sup>6</sup>  $r_d$ , ( $r_d/\lambda < 1$ ). In that case the absorption coefficient can be assumed to be

$$k_\lambda^g = (K = \lambda)\varphi, \quad (r_d/\lambda) < 1 \quad (1)$$

where  $K$  is a constant;  $\lambda$  is wavelength; and  $\varphi$  is the volume fraction of particles in the gas-particle medium. Equation (1) is an absorption coefficient that fits the emittance results for soot-containing gases.<sup>1,7</sup> For the emission temperature range of interest for the GPR (300–1200 K), more than 90% of the radiation will be in the range  $1 \leq \lambda \leq 75 \mu\text{m}$ . Therefore, the particles must satisfy  $r_d < 1 \mu\text{m}$ . As mentioned previously, it was assumed that the gas and particles are at the same temperature. The conditions for the validity of this approximation are presented in Ref. 6.

An important part of the  $\epsilon_T$  calculation is the window specular transmission,  $\tau_\lambda^w$ . For most window materials  $\tau_\lambda^w$  can be approximated as a constant,  $\tau_w$ , within a prescribed wavelength range,  $\lambda_t \leq \lambda \leq \lambda_u$ , and  $\tau_\lambda^w = 0$  outside this wavelength range.<sup>8</sup> Using this window approximation and the

assumptions described previously, the following result is obtained for  $\epsilon_T$ .<sup>6</sup>

$$\epsilon_T = \tau_w F(\lambda_u T_p) \quad (2)$$

For the condition

$$\gamma = (3.6 K k T_p / hc) \varphi D > 1 \quad (3)$$

where

$$F(x) = \frac{2\pi hc^2}{\sigma} \int_0^x \frac{du}{u^5 [\exp(hc/ku) - 1]} \quad (4)$$

The quantity  $F(x)$  is tabulated in Ref. 1. Other quantities appearing in Eqs. (2) and (3) are the speed of light  $c$ , Planck's constant  $h$ , Boltzmann's constant  $k$ , ( $hc/k = 14,388 \mu\text{m} \cdot \text{K}$ ), and the Stefan Boltzmann constant  $\sigma = (5.67 \times 10^{-8} \text{ W/M}^2 \text{K}^4)$ . In Fig. 2,  $\epsilon_T/\tau_w$  is shown as a function of  $\lambda_u T_p$  for  $\gamma > 1$ . For large  $\lambda_u T_p$ ,  $\epsilon_T$  will depend only on the window transmission.

Consider the volume fraction  $\varphi$  necessary to attain large  $\gamma$  ( $> 1$ ). The parameter  $K$  is in the range  $4\text{--}6 \mu\text{m}/\mu\text{m}$  for soot.<sup>1</sup> Therefore, assume  $K \approx 5 \mu\text{m}/\mu\text{m}$ . Also, considering the lowest temperature of interest  $T_p \approx 300 \text{ K}$  and again using  $D \approx 1 \text{ cm}$  the volume fraction necessary to attain  $\gamma > 1$  is  $\varphi > 2.7 \times 10^{-4}$ .

Based on the preceding discussion,  $\varphi > 10^{-4}$  should insure the maximum feasible emissivity. However, as Fig. 2 shows, only for  $\lambda_u T_p \geq 7 \times 10^3 \mu\text{m} \cdot \text{K}$  will  $\epsilon_T/\tau_w$  be large ( $\epsilon_T/\tau_w > 0.8$ ). At  $T_p \approx 300 \text{ K}$  this means  $\lambda_u \geq 20 \mu\text{m}$ . There are few materials with good transmission at wavelengths this long. Therefore, the GPR will be more appropriate for higher temperatures.

As discussed, it is the window transmission that determines the GPR emissivity. Therefore, it is critical to have a window with large transmittance in the wavelength range of interest. Since the radiator temperatures of interest are 300–1200 K the majority of emitted radiation will be in the infrared ( $\lambda > 1 \mu\text{m}$ ). Therefore, window materials such as ordinary glass will not be

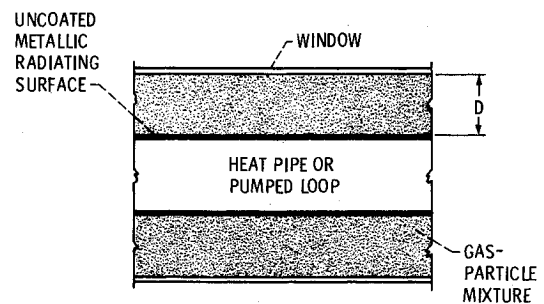


Fig. 1 Gas particle radiator concept.

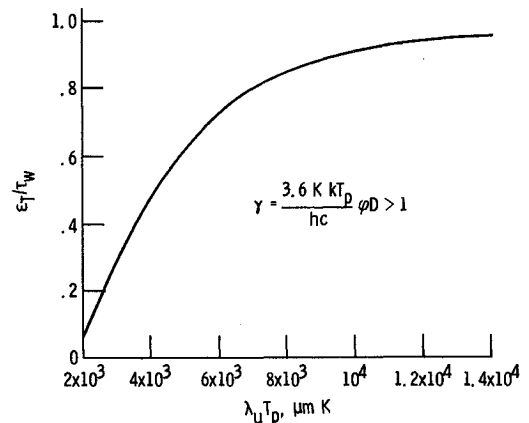


Fig. 2 Total emissivity for small particles ( $r_d < 1 \mu\text{m}$ ,  $T_p \leq 1200 \text{ K}$ ).

suitable. The alkali halides such as NaCl, NaF, and CsBr have excellent transmittance in the infrared. Also, the heavy-metal fluoride glasses<sup>9</sup> are excellent infrared transmitters. Manufacturing large pieces of these materials of the required optical properties may be a problem. However, continuous single crystal fibers of cesium bromide and other alkali halides with excellent transmittance have been manufactured.<sup>10</sup> A list of infrared transmitters and their properties is given in Ref. 6.

### Mass Comparison between Gas Particle Radiator and Tube Radiator

Assume that the total radiator mass is proportional to the radiator surface area. Then the ratio of the mass of a GPR,  $M_T$ , to the mass of the tube-type radiator,  $M_0$ , is the following

$$M_T/M_0 = a_T A_T / a_0 A_0 \quad (5)$$

where  $a$  is the proportionality constant.

The area ratio,  $A_T/A_0$ , is determined by the power radiated. For a space radiator, redundant area must be included to make up for radiator area lost as a result of meteoroid penetration. As mentioned in the Introduction, the window for the GPR acts as a bumper to protect the radiator surface. Therefore, if the window is penetrated by a meteoroid the radiating gas particle mixture is lost but the radiator surface will remain operable. This remaining surface will have an emissivity  $\epsilon'_T$  that is less than the GPR emissivity,  $\epsilon_T$ . For the tube-type radiator all area that is affected by a meteoroid penetration is lost as a radiating surface. The radiator area  $A_s$  with emissivity  $\epsilon_0$  that remains operative at the end of the mission must be sufficient to emit the entire radiator load. In the case of the GPR the radiator load at the end of the mission is shared by two areas. They are the area  $A_s$  with emissivity  $\epsilon_T$  that does not suffer meteoroid penetration, and the area  $A_T - A_s$  with emissivity  $\epsilon'_T$  that has lost the gas particle mixture as a result of meteoroid penetration. If both the GPR and the tube-type radiator are operating with the same load and with the same view factor, the following relation is obtained for the ratio,  $A_T/A_0$ :

$$A_T/A_0 = \epsilon_0/\epsilon_T \left[ 1 + \frac{\epsilon'_T}{\epsilon_T} \left( \frac{1}{r} - 1 \right) \right]^{-1} \quad (6)$$

In obtaining Eq. (6) the same redundancy factor  $r$  was assumed for the GPR and the tube-type radiator:

$$r = A_s/A_T = A_{s0}/A_0 \quad (7)$$

In Ref. 6 an expression for  $a_T/a_0$  is developed. This parameter is most sensitive to the thickness of the radiator tube of the GPR,  $t_p$ , the thickness of the radiator tube of the tube-type radiator,  $t_0$ , the window thickness,  $t_w$ , of the GPR and the thickness of the connecting member between the plate and window of the GPR  $t_s$ .

Since the window of the GPR acts as a bumper against meteoroid penetration of the radiating surface the total thickness,  $t_p + t_w$ , can be significantly less than  $t_0$  and still provide the same meteoroid protection. For high speed meteoroids ( $\sim 20$  km/s) the bumper fragments and vaporizes the meteoroid dispersing the fragments over a large area so that penetration of the main wall does not occur. Data from Explorer 46<sup>3</sup> using a stainless steel bumper and main wall indicated that  $t_p + t_w \approx t_0/6.9$  provided the same meteoroid protection as  $t_0$ . In this case,  $t_w$  is the bumper thickness. Since meteoroid penetration depth is not sensitive to the target material,<sup>11,12</sup> it is expected that similar behavior will exist for other material. In Ref. 3 the optimum distribution of mass

between the bumper and the main wall was calculated to be  $t_w/t_p = 0.1-0.2$ . Using this result together with  $t_p + t_w = t_0/6.9$  the following is obtained:

$$0.12 \leq t_p/t_0 \leq 0.13 \quad (8)$$

Now consider a comparison between a proposed heat-pipe radiator<sup>12</sup> and a hypothetical GPR. The heat pipe radiator of Ref. 12 uses a flat plate radiating surface of titanium at  $T_p = 775$  K with an emissivity,  $\epsilon_0 = 0.9$  and a total radiated power of 1.01 MW. The radiator wall thickness ( $t_0 = 0.60$  mm) and redundancy ( $r = 321/360$ ) was designed to provide a lifetime of seven years with 0.99% probability of survival against meteoroid penetration. The emitting gas particle mixture for the hypothetical GPR consists of small carbon particles and helium. The conditions necessary to insure that  $\gamma > 1$  and that negligible temperature difference exists between the particles and gas are developed in Ref. 6.

Window material was chosen to obtain high emissivity. From Fig. 2 it can be seen that  $\lambda_u T_p \geq 10^4$   $\mu\text{m K}$  for  $\epsilon_T/\tau_w \geq 0.9$ . Therefore, for  $T_p = 775$  K,  $\mu_u \geq 13$   $\mu\text{m}$ . There are several materials<sup>6</sup> that satisfy  $\lambda_u \geq 13$   $\mu\text{m}$  and also have a melting point significantly above 775 K. For the hypothetical GPR sodium chloride was chosen as the window material. For NaCl<sup>8</sup>  $\lambda_u = 15$   $\mu\text{m}$  and  $\tau_w > 0.9$ . Using Fig. 2 for  $\lambda_u T_p = 1.16 \times 10^4$   $\mu\text{m K}$ , and  $\tau_w = 0.9$  results in  $\epsilon_T = 0.84$ . Thus  $\epsilon_T$  is slightly less than the assumed emissivity  $\epsilon_0 = 0.90$ , of the heat pipe radiator. When the area ratio  $A_T/A_0$  [Eq. (6)] is calculated using  $\epsilon'_T = 0.3$  and  $r = 321/360$  however, it is found that  $A_T/A_0 = 1.03$ . The increase in area resulting from  $\epsilon_0/\epsilon_T > 1$  is nearly compensated for by the redundant area savings  $[1 + \epsilon'_T/\epsilon_T (1/r - 1)]^{-1}$  term in Eq. (6).

As already mentioned, the thickness of the heat pipe wall is  $t_0 = 0.6$  mm. Applying Eq. (15) results in  $0.072 < t_p < 0.078$  mm. Although it may be possible to use such a thin wall thickness,  $t_p = 0.1$  mm was arbitrarily chosen as a practical limit on  $t_p$ . This same limit was also chosen for  $t_w$ , so that  $t_w = t_p = 1/6$   $t_0 = 0.1$  mm. With  $t_w + t_p = 0.2$  mm meteoroid protection will be more than required ( $t_w + t_p \approx t_0/6.9$ ). Titanium of thickness  $t_s = t_p = 0.1$  mm was also assumed for the connecting member between the plate and window.

Using the materials, wall thicknesses, and dimensions already described, the specific mass ratio  $a_T/a_0$  was calculated<sup>6</sup> and found to be 0.67. From this result plus  $A_T/A_0 = 1.03$ , Eq. (5) yields  $M_T/M_0 = 0.69$ . Thus the GPR results in a 31% mass reduction from the comparable heat pipe radiator.

### Conclusion

This study was directed at predicting the performance of a new space radiator concept, the gas particle radiator (GPR). The GPR uses a gas containing submicron particles as the radiating media. The gas particle mixture is contained between the radiator's emitting surface and a transparent window. The GPR has two major advantages over conventional heat-pipe or pumped loop radiators. First, high emissivity is achieved without the use of emissive coatings. Second, the GPR potentially has a lower mass.

For a modest volume fraction ( $\phi > 10^{-4}$ ) of submicron particles and gas thickness ( $D \approx 1$  cm) it was found that the emissivity was determined by the window transmittance. Thus the window becomes a critical element in the GPR concept. The window must have high transmittance in the infrared and be structurally strong enough to contain the gas particle mixture. In addition, the window acts as a "bumper" to provide meteoroid protection for the radiator wall. This results in lower mass for the FPR.

The GPR was compared to a proposed titanium wall, potassium heat pipe radiator. For both radiators operating at a power level of 1.01 MW at 775 K it was found that the GPR mass was 31% lower than the heat pipe radiator.

## References

- <sup>1</sup>Siegel, R. and Howell, J. R., *Thermal Radiation Heat Transfer*, 2nd ed., Hemisphere, New York, 1981.
- <sup>2</sup>Lundeberg, J. F., Stern, P. H., and Bristow, R. J., "Meteoroid Protection for Spacecraft Structures," D2-25056, Boeing Co., Seattle, WA, Oct. 1965, (NASA CR-54201).
- <sup>3</sup>Humes, D. H., "Meteoroid Bumper Experiment on Explorer 46," NASA TP-1879, 1981.
- <sup>4</sup>Lanzo, C. D. and Ragsdale, R. G., "Experimental Determination of Spectral and Total Transmissivities of Clouds of Small Particles," NASA TN D-1405, NASA Lewis Research Center, Hampton, VA, 1962.
- <sup>5</sup>Howell, J. R. and Renkel, H. E., "Analysis of the Effect of a Seeded Propellant Layer on Thermal Radiation in the Nozzle of a Gaseous-Core Nuclear Propulsion System," NASA TN D-3119, NASA Lewis Research Center, Hampton, VA, 1965.
- <sup>6</sup>Chubb, D. L., "Analysis of the Gas Particle Radiator," NASA TM-88786, NASA Lewis Research Center, Hampton, VA, 1986.
- <sup>7</sup>Siegel, R., "Radiative Behavior of a Gas Layer Seeded with Soot," NASA Lewis Research Center, Hampton, VA, NASA TN D-8278, 1976.
- <sup>8</sup>Touloukian, Y. S. and DeWitt, D. P., *Thermophysical Properties of Matter*, Vol. 8, Thermal Radiative Properties, Nonmetallic Solids, Plenum, New York, 1972.
- <sup>9</sup>Drexhage, M.G. and El-Bayoumi, O. H., "Heavy-Metal Fluoride Glasses for Mid-IR Military Applications," *Aerospace America*, Vol. 23, No. 4, April 1985, pp. 66-69.
- <sup>10</sup>Mimura, Y., Okamura, Y. and Ota, C., "Single-Crystal CsBr Infrared Fibers," *Journal of Applied Physics*, Vol. 53, No. 8, Aug. 1982, pp. 5491-5497.
- <sup>11</sup>"Frost, V.C., Meteoroid Damage Assessment," NASA SP-8042, Washington DC, 1970.
- <sup>12</sup>Girrens, S. P., "Design and Development of a Titanium Heat-Pipe Space Radiator," Los Alamos Rept., LA-9251-MS, Los Alamos, NM, March 1982.

## TO APPEAR IN FORTHCOMING ISSUES OF THIS JOURNAL

**Assessment of Two-Temperature Kinetic Model for Dissociating and Weakly-Ionizing Nitrogen** by C. Park.

**Monte Carlo Simulations in Support of the Shuttle Upper Atmospheric Mass Spectrometer Experiment** by J.N. Moss and G.A. Bird.

**Steady State Ablation of an Arrhenius Material by External Heating** by W. Borsch-Supan and L.W. Hunter.

**Transient Response of a Liquid Metal Heat Pipe** by D.E. Tilton, L.C. Chow, and E.T. Mahefkey.

**Roll-Out-Fin Expandable Space Radiator Concept (TN)** by R. Ponnappan, J.E. Beam, and E.T. Mahefkey.

**Fluid Loss from a Puncture of a Space Radiator** by D.E. Tilton and L.C. Chow.

**Solar Energy Transfer Through Semi-Transparent Plate Systems** by S.J. Mitts and T.F. Smith.

**Heat Transfer and Pressure Drop Experiments in Aircooled Electronic Component Arrays** by W.F.N. Santos and P.R.S. Mendes.

**Conjugated Heat Transfer from a Strip Heater with Unsteady Surface Element Method** by K.D. Cole and J.V. Beck.

**An Experimental Study of the Transient Contact Conductance and the Temperature Distribution in Periodically Contacting Surfaces** by W.M. Moses and R.R. Johnson.

**Transient, Stratified, Enclosed Gas and Liquid Behavior with Concentrated Heating from Above** by B. Abramzon, D.K. Edwards, and W.A. Sirignano.

**Natural Convection along a Wedge** by L.S. Yao.

**Thermal Boundary Layer on a Continuous Moving Plate with Freezing** by F.-B. Cheung.

**Condensation Heat Transfer in a Microgravity Environment (TN)** by L.C. Chow and R.C. Parish.

**Radiative Shape Factors Between Differential Ring Elements on Concentric Axisymmetric Bodies** by M.F. Modest.

**Radiative View Factors from Differential Plane Sources to Disks—A General Formulation** by M.H.N. Naraghi.

**Radiative Transfer in Thermal Insulations of Hollow and Coated Fibers** by K.Y. Wang, S. Kumar, and C.L. Tien.

**Successful Improvement of the Modified Differential Approximation in Radiative Heat Transfer** by C.Y. Wu, W.H. Sutton, and C.F. Love.

**Heat Transfer by Combined Conduction and Radiation in Axisymmetric Enclosures** by A. Yücel and M.L. Williams.

**Crystallographic Effects During Radiative Melting of Semitransparent Materials** by B. W. Webb and R. Viskanta.

**Two Wavelength Holographic Measurements of Temperature and Concentration during Alloy Solidification** by A. Ecker.